Behavior of Beta Amyloid 1-16 at the Air-Water Interface at Varying pH by Nonlinear Spectroscopy and Molecular Dynamics Simulations

Abigail E. Miller[¶1#], *Poul B. Petersen*[1†], *Christopher W. Hollars*[¶§], *Richard J. Saykally*[1]*
[1]Department of Chemistry, University of California, Berkeley, CA 94720-1460;
[¶]Chemistry, Materials, and Life Science Directorate, Lawrence Livermore National Laboratory, Livermore, CA 94550

Jan Heyda,[2] *Pavel Jungwirth*[2*]
[2]Institute of Organic Chemistry and Biochemistry, Academy of Sciences of the Czech Republic, and Center for Biomolecules and Complex Molecular Systems. Flemingovo nám. 2,16610 Prague 6, Czech

Corresponding authors: saykally@berkeley.edu (RJS) and pavel.jungwirth@uochb.cas.cz (PJ)

[§]present address: Midwest Research Institute, Kansas City, MI 64110; †present address: Department of Chemistry, Massachusetts Institute of Technology Cambridge, MA 02139; [#]present address: Physics Laboratory, National Institute of Standards and Technology, Gaithersburg, MD 20899

Keywords: Second harmonic generation, beta amyloid, Brewster Angle Microscopy, surface adsorption

Abstract. The adsorption and aggregation of beta amyloid (1-16) fragment at the air/ water interface was investigated by the combination of second harmonic generation (SHG) spectroscopy, Brewster angle microscopy (BAM), and molecular dynamics simulations (MD). The Gibbs free energy of surface adsorption was measured to be -10.3 kcal/mol for bulk pHs of 7.4 and 3, but no adsorption was observed for pH 10-11. The 1-16 fragment is believed not to be involved in fibril formation of the beta amyloid protein, but it exhibits interesting behavior at the air/water interface, as manifested in two time scales for the observed SHG response. The shorter time scale (minutes) reflects the surface adsorption, and the longer time scale (hours) reflects rearrangement and aggregation of the peptide at the air-water interface. Both of these processes are also evidenced by BAM measurements. MD simulations confirm the pH dependence of surface behavior of the beta amyloid, with largest surface affinity found at pH = 7. It also follows from the simulations that phenylalanine is the most surface exposed residue, followed by tyrosine and histidine in their neutral form.

Introduction

Alzheimer's disease(AD) is a neurological disorder characterized by the formation of insoluble plaques comprising fibrils of aggregated beta amyloid protein[1,2]. The fibrils are thought to be primarily composed of the first 43 residues of the beta amyloid protein as a peptide fragment that has structurally rearranged from a random coil and alpha helix conformation into a beta sheet[3]. The latter half of the beta amyloid peptide (residues 25-35) is sufficient for fibril formation[4,5] but it is presently unknown how the first half of the beta amyloid fragment is involved in the process. More recent studies, briefly reviewed in Ref 6, have implicated the formation of soluble oligomers of beta amyloid, rather than insoluble fibrils, as a key element in the pathogenesis of AD.

Interfaces constitute sites that can catalyze or otherwise influence chemical processes like aggregation. Numerous studies, including recent work investigating ions at the air-water interface, have demonstrated the utility of second harmonic generation (SHG) for probing the surface behavior of ions and molecules[7,8]. SHG is a nonlinear optical process that is the result of two photons of the same energy being converted by a non-centrosymmetric medium into a single photon of twice the energy. This requirement of broken inversion symmetry within the dipole approximation makes SHG a surface-specific technique for bulk centrosymmetric samples, e.g. aqueous solutions, and it can be used to determine interfacial concentrations of molecules through resonant enhancement of the SHG response via their respective absorption spectra. Some earlier SHG studies have been done on proteins at the air-water interface. Girault and coworkers investigated glucose oxidase[9], cytochrome c[10,11], hemoglobin and myoglobin[12] exploiting the SHG response of specific chromophores, while other groups have examined

tryptophan peptides[13-15]. SHG circular dichroism has been used to investigate the molecular orientation of proteins at interfaces[16-18].

Beta amyloid fibrils form on neurons. Since the water structures at water-hydrophobe and water-air interfaces are thought to be similar, the study of aggregation of beta amyloid at the air/water interface can lend some insight into its interfacial behavior, and has previously been investigated experimentally [4,19-23]. Eisenthal and Salafsky measured the absorption of beta amyloid 1-40 to a silica/water interface[11], but the quantitative affinity of beta amyloid for an air-water interface, and the role **of** the first half of the beta amyloid peptide at the interface have not yet been established. Also, despite a large body of simulation studies of beta amyloids including their interaction with anti-aggregation agents and various interfaces,[24-29] the behavior at the water surface has been explicitly addressed only for model amyloids or amyloid-like hydrophobins [30-32]. In the present paper we investigate the surface behavior of the first half of the beta amyloid peptide by means of SHG spectroscopy and molecular dynamics (MD) simulations, augmented by BAM measurements.

Materials and Experimental Methods

For the SHG studies, beta amyloid 1-16 (Anaspec, Inc) was dissolved in buffer at 1 mg per 25 mL buffer. To achieve pH 7, two different buffers were used: phosphate buffered saline (0.01 M PBS, which is 0.138 M NaCl, 0.0027 M KCl, 0.02% N_3; pH 7.4) and citrate (0.05 M citrate, 0.001 M $NaHPO_4$, pH 7). Carbonate buffer (0.05 M K_2CO_3, 0.04 M $KHCO_3$) produced a pH of 10 and pH 3 was achieved with a phosphate buffer (0.05 M $KHPO_4$, 0.006 M HCl). All salts were purchased from Sigma-Aldrich and the water was

produces in a Millipore system generating 18.2 MΩ with < 4 ppm total organic content (Millipore, MilliQ gradient). Beta amyloid 1-16 (Anaspec, Inc) was also dissolved in water at 1 mg per 25 mL 18.2 MΩ water with concentrated HCl (Sigma-Aldrich) added to reach pH 3 and concentrated NaOH (Sigma-Aldrich) added to reach pH 11. All glassware was washed with Nochromix (a hot chromic acid substitute) and rinsed with 18.2 MΩ water. All dilutions were made 20-30 minutes before measurements, which were done on 20 mL of solution in a Petri dish enclosed in a box in air with a gentle air flow to circulate the surface without generating waves.

The optical system employed to probe the interfacial peptide concentrations is based on an amplified femtosecond laser system driving an UV second harmonic generation spectrometer and has been previously described[7]. Briefly, ~100 fs pulses are produced at 400 nm through frequency doubling of a 800 nm Ti:sapphire laser system operating at a repetition rate of 1 kHz. The 400 nm beam is focused onto the sample and the second harmonic at 200 nm is filtered and spatially separated from the fundamental by a fused silicon prism and detected by a solar blind photomultiplier. All data were collected with boxcar integration and processed in custom written programs for LABVIEW then analyzed and fit in IGOR PRO, as described in Ref. 6.

For the BAM studies, 1 mg of beta amyloid 1-16 (Anaspec, Inc) was dissolved in 25 mL of PBS buffer, pH 7.4. The Brewster angle microscope (BAM2plus, Nanofilm Technologies GmbH, Goettingen, Germany) was operated with a Nd:YAG laser in a enclosed box. Each image was collected for 30 s.

The absorption spectra were measured using 400 μL of solution in a quartz cuvette (Perkin Elmer, Waltham, MA) with a 1 cm pathlength in a UV/Vis spectrometer (Cary 300, Perkin Elmer, Waltham, MA).

Computational Methods

MD simulations were performed in order to investigate computationally the surface activity of the beta-amyloid as a function of pH. As in the experiment, acidic (pH=3), neutral (pH=7), and basic (pH=10) conditions were simulated. In the beta-amyloid (i.e., polypeptide H_2N-DAEFRHDSGYEVHHQK-COOH) the titratable groups (i.e., K, R, H, D, E, Y, and the terminal groups) were either charged or neutral according to apparent pKa values.[33] The protonation states were established for each of the investigated values of pH using the program PropKa[34] and are presented in Table 1. It should be noted here, that the pKa values are to some extent structure dependent (due to presence of salt bridges, backbone-sidechain H-bonds, electrostatic repulsion or attraction and local desolvation) so that for acidic and basic pH the overall charge may vary by up to one unit. Here, we employed values which exactly agree with the experimentally observed ones.

In order to improve sampling, two simulations with very different initial conditions were carried out for each value of pH, with one trajectory started with the beta-amyloid placed at the air-water interface and other in the middle of the slab. The total time of each trajectory was 230 ns, with the information about the initial position of the beta-amyloid being lost within the first few tens of nanoseconds. From these, the first 50 ns were discarded when calculating density profiles, i.e., averaged distributions of all

the atoms across the slab. The employed time step was 1 fs and coordinates were saved every 1 ps. By performing block averages, we checked that the simulation length was sufficient to provide converged structural results in terms of radius of gyration of the beta-amyloid.

We employed the parm99 force field for the polypeptide,[35] the SPC/E water model,[36] together with (non-polarizable) parameters for Cl^- and K^+ ions,[37] needed to compensate the net charge of the beta-amyloid. For the non-standard amino acid residues charges were evaluated using the ab initio RESP procedure as recommended for the Amber force fields.[38]

The size of the unit cell was 65 × 65 × 265 Å. 3D periodic boundary conditions were applied with long-range electrostatic interactions beyond the nonbonded 9Å cutoff accounted for using the particle mesh Ewald (PME) method.[39] The Berendsen temperature (300 K) coupling was employed,[40] and all bonds containing hydrogens were constrained using the SHAKE algorithm.[41] All MD simulations were performed using the Amber 10 program.[38]

Results and Discussion

Experimental

Beta amyloid (1-16) has UV absorption maxima at both 220 nm, due to the peptide backbone, and at 280 nm due to the amino acid side chains (Figure 1). For the second harmonic generation (SHG) study, the backbone absorption was exploited because it is much stronger, and the available laser power is higher and more stable at (pump wavelengths) 400 nm than near 560 nm. Although the phosphate ions in the buffer

begin to absorb at 200 nm, those absorptions are much weaker than that of the amyloid at 200 nm (Figure 1), and the buffer is kept at a constant concentration throughout the experiment, thereby producing a constant background SHG signal. Changes in the SHG intensity with bulk concentration and/or time are therefore attributed to amyloid absorption to the air-water interface. The SHG response from the peptide is normalized to the background signal from the buffer so that all graphs comprise plots of relative intensity of peptide SHG response above that of buffer. By making the SHG resonant with the peptide absorption transition, the peptide and buffer responses can readily be separated, again noting that the resonant absorption from the buffer is very weak. We also note that the depth of the interface that is actually probed in an SHG experiment on complex samples is not well-defined.

The SHG response of the beta amyloid 1-16 was measured as a function of bulk peptide concentration to determine the adsorption isotherm, following standard procedures[7,8]. The second order susceptibility of the peptide is proportional to its surface concentration, and is modeled here by the standard Langmuir adsorption isotherm under the assumption of non-interacting particles[42] (Figure 2):

$$\chi^{(2)}_{peptide}/\chi^{(2)}_{buffer} \propto N_s = N_s^{max}\, C / (C + C_w \exp(\Delta G_{abs}/RT)) \qquad (1)$$

Here ΔG_{abs} is the Gibbs free energy of adsorption of the peptide to the interface , C is the bulk peptide concentration, C_w is the bulk water concentration, N_s^{max} is the maximum surface concentration and N_s is the surface concentration of the peptide. The SHG response was fit to the Langmuir model, yielding a Gibbs free energy of adsorption of -10.3 kcal/mol(±0.8) at both pH 7.4 and pH 3 (Figure 2). The reported uncertainty is one standard deviation from a fit of the data, weighted by reciprocal variences,[7,8] but the

actual uncertainty is certainly large, primarily due to the model dependence.. An attempt was made to fit the data to the amphiphilic isotherm model[42], which incorporates additional parameters describing aggregation of monomers and the interaction of charged particles, but no significant dependence was found for those parameters. Hence, the simple Langmuir model was considered sufficient for determining the free energy for the peptide adsorbing to the air-water interface. We estimate a 30% uncertaintity in our determination of this quantity.

Within our experimental precision, the free energy of adsorption for beta amyloid 1-16 is not significantly different between an acidic solution (pH 3) or neutral solution (pH 7), as shown in Figure 2, but the peptide exhibits no detectable presence at the interface in a basic solution (pH 10) at any concentration. All measurements, for determining the free energy, were taken 30 minutes after solution preparation, well before any peptide aggregation processes occur.

The buffer ions are not responsible for the partitioning of the beta amyloid 1-16 to the air-water interface. The SHG response of the peptide was measured for water without any buffer, using strong acid and base to reach pH 3 and 11, respectively, and the same response was found as for the buffered solutions (Figure 2).

At pH 7, the beta amyloid 1-16 has four negatively charged side chains and two positively charged side chains. At pH 3 there are five positively charged side chains and one that is negatively charged, whereas at pH 10 there are five negatively charged side chains and one positively charged side chain. It is probable that the charge balance of the peptide strongly affects its surface affinity, as the hydration properties of the residues

comprising the side chains vary considerably, and these are likely to be determining factors.

There appear to be two different time scales for beta amyloid 1-16 adsorption to the air-water interface. The shortest of these describes the absorption of the peptide to the interface (Figure 3), which occurs over the course of minutes. The maximum surface concentration is reached after 30 minutes for 20 μM beta amyloid 1-16, wherein the SHG signal levels off. On this shorter time scale, equilibrium between the bulk and interfacial peptide concentrations appears to have been reached. This SHG-measured time dependence for the absorption of beta amyloid 1-16 is similar to the time scale previously found for the adsorption of the full length beta amyloid protein, as determined by changes in the surface tension[47].

On a longer time scale, the SHG response exhibited further changes (Figure 4). The SHG signal decreased over the course of hours, depending on the bulk concentration of the beta amyloid 1-16. For these experiments, the first measurement was taken 30 minutes after the solution was mixed. For 20 uM beta amyloid 1-16, the maximum SHG response was already reached at t=0 and the SHG response decreased with time, reaching a minimum (Figure 4). Upon decreasing the beta amyloid 1-16 concentration to 10 μM, the t=0 SHG response began increasing and did not reach a maximum until 1 hour, whereupon it then decreased until it matched the SHG response of the 20 uM solution. For the 2.5 μM solution, the maximum SHG response occurred after 2 hours, decreasing thereafter to the same constant value as for the 20 and 10 μM solutions. The 1 μM solution showed the same trend, except that it exhibited its maximum SHG signal after 4

hours, at the same level to which the higher concentration solutions had stabilized (Figure 4). No evidence of optical damage was observed in the present measurements.

The faster time scale found here (Fig 3) can be related to saturation of the surface with peptide, because the BAM experiments described below yield a correlating result. At higher bulk concentrations, it takes less time for the air- water interface of the solution to become saturated with peptide, which is evidenced by observing the maximum SHG response on a faster time scale. The beta amyloid 1-16 comprises only 16 amino acids, which can form an alpha helix. The decrease in SHG response is likely due to the rearrangement of the beta amyloid 1-16 at the interface i.e. once the surface is saturated with the peptide, it rearranges[9]. We speculate that this rearrangement could involve an unfolding and refolding of the peptide, thereby producing a greater SHG response, since the alpha helical structure is more ordered than the unfolded structure. This contention is further supported by our BAM experiments described below.

Using Brewster angle microscopy, the saturation of the surface and rearrangement, or entanglement, of the beta amyloid 1-16 peptide was observed directly. A series of images was collected every one to two minutes after the water surface (the air-water interface) was refreshed by aspiration. A representative data set is shown in Fig. 5. The lighter color in the images is due to water and the darker colored objects in the images are the peptide domains. Initially (at time zero), there is very little peptide at the interface, but over time, more appears. After five and eight minutes, the beta amyloid 1-16 has formed entangled structures at the interface that appear stretched out. As additional peptide adsorbs to the surface, the entangled structure continues to get denser, until after around 25 minutes, bare water surface is no longer visible. Unlike previous studies of

proteins at the air-water interface[48], we do not observe a homogeneous distribution of the beta amyloid 1-16 peptide over the surface . Rather, as the peptide absorbs to the interface, it appears to form entangled domains, as described above. Due to the resolution of the microscope and the size of the peptide, the strands seen in the images cannot be due to single beta amyloid 1-16 peptides, but must result from a number of interacting peptide strands. This domain formation is also visible via SHG in terms of large fluctuations in signal that correspond to domains moving across the surface optical spot (Figure 6a, b). Distinct bursts of SHG response occur from the interfacial peptide at all concentrations. Due to air flow, the surface is not static; the peptides drift in and out of the excitation region. The fluctuations observed during the measurement of the SHG response for the buffers are a measure of the intrinsic noise of the system (Figure 6c), which is at least an order of magnitude lower than the fluctuations in SHG response attributed to the domain formation of the peptide at the air- water interface.

Recent work by Triulzi et al.[5] demonstrates a presence of beta amyloid 25-35 at the air water interface, where it was found to aggregate. Here, we demonstrate that beta amyloid 1-16, i.e. the protein amino acid sequence that induces aggregation, not only exists at the air water interface, but actually exhibits a strong preference for the interface relative to the bulk. Beta amyloid 1-16 does not form distinct, observable fibrils, but it does aggregate into domains (Figure 5). These domains created by the 1-16 section of beta amyloid may assist fibril formation by bringing the 25-35 sections of beta amyloid into close contact.

Computational

The simulated trajectories were first analyzed in terms of density profiles of all the heavy atoms, i.e., averaged distributions in the z-direction from the center of the slab to the water/vapor interface. Density profiles of heavy atoms of the beta-amyloid and water, evaluated for the three investigated pH values of 3, 7, and 10 are shown in Figure 8. We see that at pH 7 the beta amyloid strongly segregates to the water surface. In contrast, at pH 3 and 10 the polypeptide distributes almost evenly across the slab. At pH 7 the absolute value of the charge on the beta amyloid is the lowest amounting to 2e, while both at pH 3 and 10 the absolute values of the overall charge is 5e (see Table 1). We thus observe an anticorrelation between the absolute value of the charge and the surface propensity of the beta amyloid. This can be rationalized using simple Coulombic arguments – the larger the total charge the stronger the hydration (i.e., the weaker the surface affinity) of the peptide.

While averaged values are presented in Figure 8, time evolutions of density profiles are shown together with the time evolution of radii of gyration of the beta-amyloid at pH 3, 7, and 10 in Figures 9, 10, and 11. These plots carry detailed information about position, orientation, and compactness of beta amyloid during the simulations. The width of the density profile tells us to which extent the beta amyloid is extended along the z-axis and what is its approximate orientation with respect to the interface (i.e., parallel, or perpendicular). The radius of gyration allows us to additionally distinguish between compact and unfolded structures. The main message from this analysis is that the size of the peptide does not change significantly when exposed at the interface compared to the situation in the aqueous bulk.

We also plotted the z-profiles at different pHs for individual amino acids (which were grouped with respect to their polarity, i.e., hydrophobic, polar, and charged residues). Due to the large number of polar and charged residues, the surface affinity of the hydrophobic residues was reduced by the presence of their polar or even charged environment. The most surface active amino acid was found to be phenylalanine, as shown in Figure 12. PHE was consistently the residue lying closest to the interface, once the beta-amyloid reached the surface region. Other, less hydrophobic amino acids (glycine, alanine, and valine) did not exhibit such a strong surface exposure. However, as the pH was varied, aromatic residues (TYR and HIS) showed, when uncharged, surface exposure similar to PHE. However, this surface affinity disappeared once these amino acids became charged. The same behavior was also apparent from calculations of solvation properties of hydrophobic residues, either by evaluating the solvent accessible surface (SAS) or the number of water molecules around each residue.

Conclusions

In conclusion, our SHG experiments have shown that beta amyloid 1-16 exhibits a large free energy of interfacial adsorption of -10.3 kcal/mol at both acidic and neutral bulk pH, but interestingly, it exhibits no presence at the air-water interface in a strongly basic solution. The peptide forms entangled domains and strands at the interface, but no beta amyloid fibril formation was observed. The beta amyloid 1-16 peptide exhibits absorption and reorganization at the interface on very different time scales. It takes longer than our experimental time to actually generate fibrils[1], but the domains formed could comprise nucleation sites for subsequent fibril formation. The strong pH dependence of surface behavior of the beta amyloid was also confirmed by MD simulations, which show

that it anticorrelates with the overall charge of the peptide. The largest surface affinity was observed at pH = 7, with little surface exposure at pH 10 and 3. The first two findings are in agreement with the SHG experiment, however, simulations do not support strong surface affinity in the third case. It is possible that increased interfacial ordering of the peptide occurs at low pH values, which would also enhance the SHG transition strengths, and this effect is not captured in the MD simulations.

Acknowledgements

This material is based upon work supported by the National Science Foundation under Grant No. 0650950. AEM was supported by a LLNL Student Employee Graduate Research Fellowship. We thank Andy Malec for use of the BAM, the Groves lab for the UV/Vis spectrometer, and Dale Otten for discussion. JH thanks the International Max-Planck Research School. PJ acknowledges support from the Czech Science Foundation (grant 203/08/0114), the Czech Ministry of Education (grant LC 512), and the Academy of Sciences (Praemium Academie).

Table 1: Protonation stated of individual amino acids of the beta-amyloid at different values of pH.

	H	Asp	Ala	Glu	Phe	Arg	His	Asp	Ser	Gly	Tyr	Glu	Val	His	His	Gln	Lys	OH	total charge
charge	0, 1	-1, 0	X	-1, 0	X	0, 1	0, 1	-1, 0	X	X	-1, 0	-1, 0	X	0, 1	0, 1	X	0, 1	-1, 0	
pKa - tabulated	8	4	X	4.4	X	13	6.3	4	X	X	9.6	4.4	X	6.3	6.3	X	10	3.8	
pKa - calculated	7.4	2.9	X	4.2	X	12.1	6.3	3.6	X	X	10.2	4.3	X	6.3	6.3	X	10	3.3	
pH=3	1	-1	X	0	X	1	1	0	X	X	0	0	X	1	1	X	1	0	5
pH=7	1	-1	X	-1	X	1	0	-1	X	X	0	-1	X	0	0	X	1	-1	-2
pH=10	0	-1	X	-1	X	1	0	-1	X	X	-1	-1	X	0	0	X	0	-1	-5

Figure Captions

Figure 1: Absorption spectra of solutions used. PBS buffer pH 7.4 (- - - -) and PBS buffer pH 7.4 with beta amyloid 1-16(------) are shown in blue, which establishes the wavelengths at which the beta amyloid 1-16 absorbs. Spectra of the salts, sodium citrate, monopotassium carbonate, dipotassium carbonate, monosodium phosphate, used to make the different pH buffers are shown with dashed lines(- - - -); the same salts with beta amyloid 1-16 present are shown with solid lines(----). See legend for absorption spectral assignments

Figure 2: Determination of the free energy of adsorption for beta amyloid 1-16 using the Langmuir model at pH 7.4 in PBS(■), at pH 10 in carbonate(♦), and at pH 3 in phosphate (▼) buffers. The SHG signals of the amyloid solutions are normalized to the respective buffers, and all fits were performed with T= 298 K. At pH 10 in carbonate buffer, there is no response above the buffer background. The fitted value of the free energy of adsorption for beta amyloid 1-16 is -10.3 (±0.8) kcal/mol at both neutral and acidic pHs. The uncertainty corresponds to one standard deviation in the weighted(by reciprocal varience) fit, according to the procedure specified in Ref 6.

Figure 3: Short-time dependence of beta amyloid 1-16 adsorption to the air-water interface at 20 μM bulk concentration. Initial surface saturation (equilibrium) is achieved after 30 minutes. The two traces are from two separate experiments performed under similar conditions. The error bars in the y-direction are the standard deviations of the

measured SHG signal. The error bars in the x direction represent the time span over which that value was measured.

Figure 4: Long time dependence of beta amyloid 1-16 adsorption to the air-water interface as a function of peptide concentration. Concentrations of 20, 10, 2.5 and 1 μM are shown as a function of time (over hours). There are three phases of adsorption at each concentration and their separation is dependent on concentration. The short time dependence is not visible in the 20 μM but is at the lower concentrations. The short time rise is followed by a depression of the SHG response related to rearrangement of the peptide at the air-water interface. Finally, there is a flattening of the SHG response as the peptide reaches an equilibrium state. All lines are to guide the eye.

Figure 5: BAM images of beta amyloid 1-16 adsorbed to the air-water interface. All images were of 20uM beta amyloid 1-16 in PBS buffer (30s exposures at 50% power). Images correspond to times for peptide adsorption to the air-water interface a) t=0 min, b) t=5 min, c) t=8 min, d) t=13 min, and e) t=25 min. The dark strands in the images are the beta amyloid 1-16. The entanglement of the peptide is evident in the strand formation visible on the micron scale.

Figure 6: Histograms of SHG signal as a function of time. Fluctuations in the first two histograms are due to peptide domains at the air-water interface moving through the laser spot. (1000 shots per bin at a 1 kHz rep rate) The last histogram has no peptide at the interface so all fluctuations are due to the system noise. a) 20 μM beta amyloid 1-16 pH 3

b) 2.5 μM beta amyloid 1-16 pH 3 and c) 1.25 μM beta amyloid 1-16 pH 10. At pH 10 there is no peptide at the interface as measured by SHG.

Figure 7: Number density profiles from MD simulations for all heavy atoms of beta-amyloid at pH=3, 7, and 10, symmetrized with respect to the middle of the slab and averaged over two initial conditions. The beta-amyloid profile is in red, and the profile of water is in blue. GDS stands for the Gibbs dividing surface.

Figure 8: Time evolution of number density profiles of all heavy atoms (averaged always over 1ns block and color-coded) together with the radius of gyration for the beta-amyloid at pH=3. The right figure corresponds to the beta-amyloid initially in the bulk, while the left figure corresponds to interfacial initial condition.

Figure 9: Same as Figure 9, but for pH = 7.

Figure 10: Same as Figure 9, but for pH = 10.

Figure 11: Time evolution of number density profile of all heavy atoms of individual amino acids of beta-amyloid at pH=10, initially placed in interfacial region. Note the largest surface affinity of phenylalanine (when the peptide is at the interface).

Figure 1

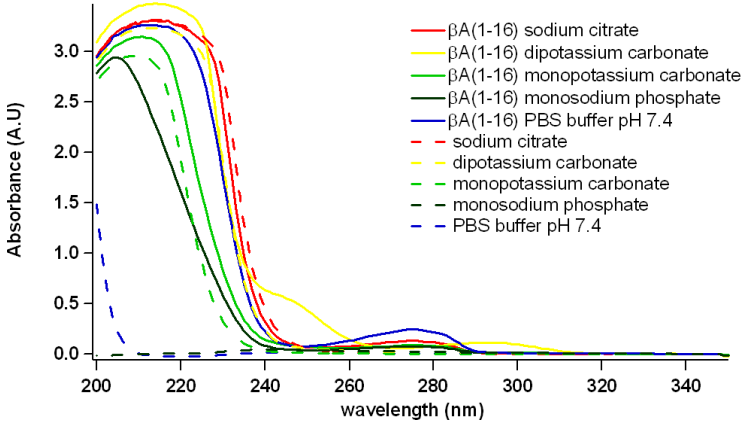
βA(1-16) sodium citrate
βA(1-16) dipotassium carbonate
βA(1-16) monopotassium carbonate
βA(1-16) monosodium phosphate
βA(1-16) PBS buffer pH 7.4
sodium citrate
dipotassium carbonate
monopotassium carbonate
monosodium phosphate
PBS buffer pH 7.4
Absorbance (A.U)
wavelength (nm)
0.0
0.5
1.0
1.5
2.0
2.5
3.0
200
220
240
260
280
300
320
340

Figure 2

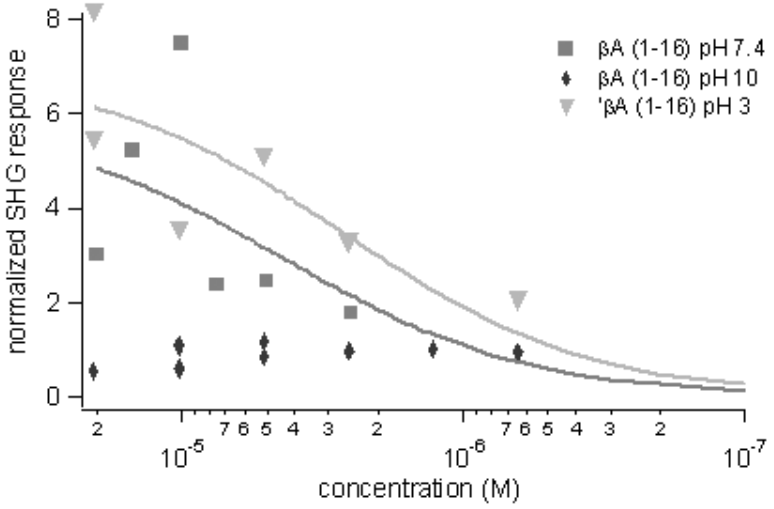
normalized SHG response
8
6
4
2
0
βA (1-16) pH 7.4
βA (1-16) pH 10
'βA (1-16) pH 3
2
7 6 5 4 3 2
7 6 5 4 3 2
10-5
10-6
10-7
concentration (M)

Figure 3

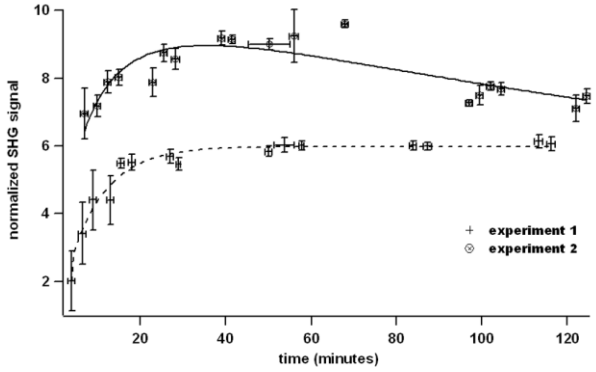
normalized SHG signal
time (minutes)
experiment 1
experiment 2
10
8
6
4
2
20
40
60
80
100
120

Figure 4

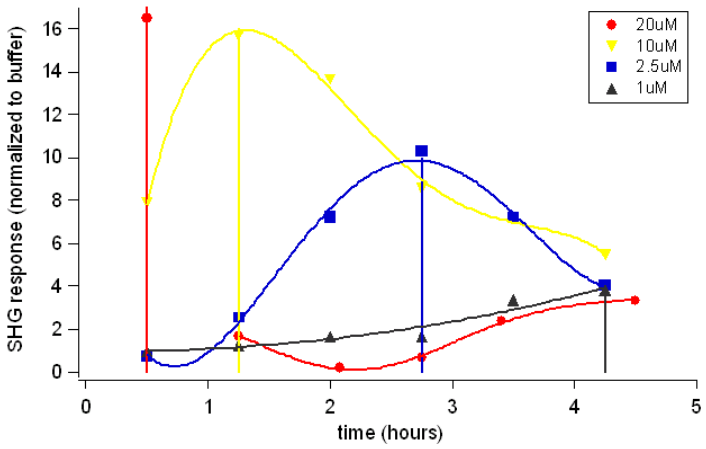
20uM
10uM
2.5uM
1uM
SHG response (normalized to buffer)
time (hours)
0
2
4
6
8
10
12
14
16
0
1
2
3
4
5

Figure 5

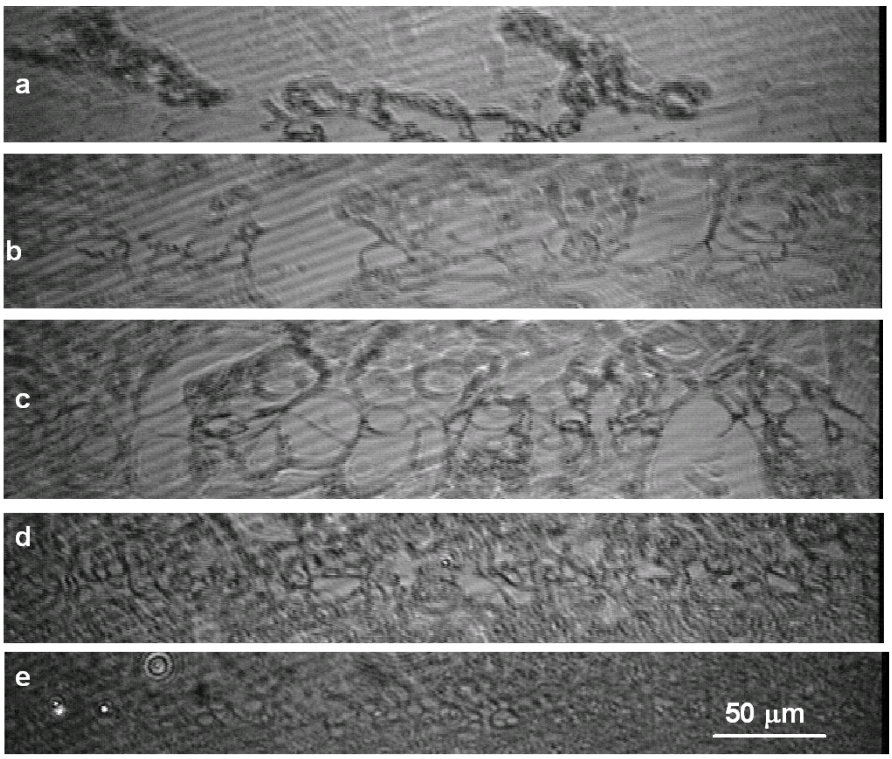

Figure 6

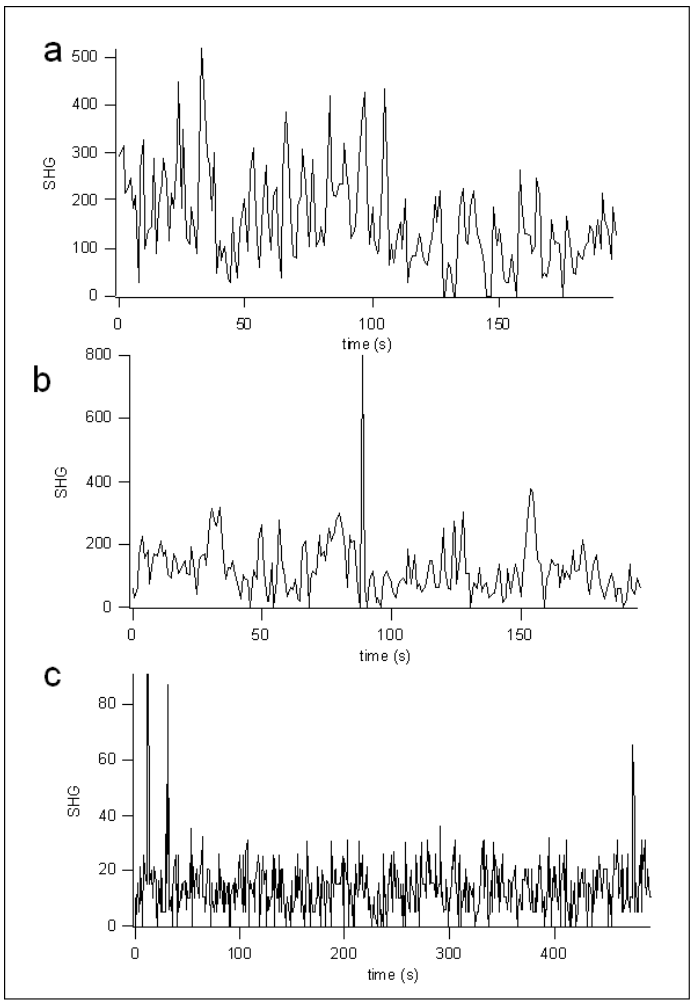
a
SHG
500
400
300
200
100
0
0
50
100
150
time (s)
b
SHG
800
600
400
200
0
0
50
100
150
time (s)
c
SHG
80
60
40
20
0
0
100
200
300
400
time (s)

Figure 7

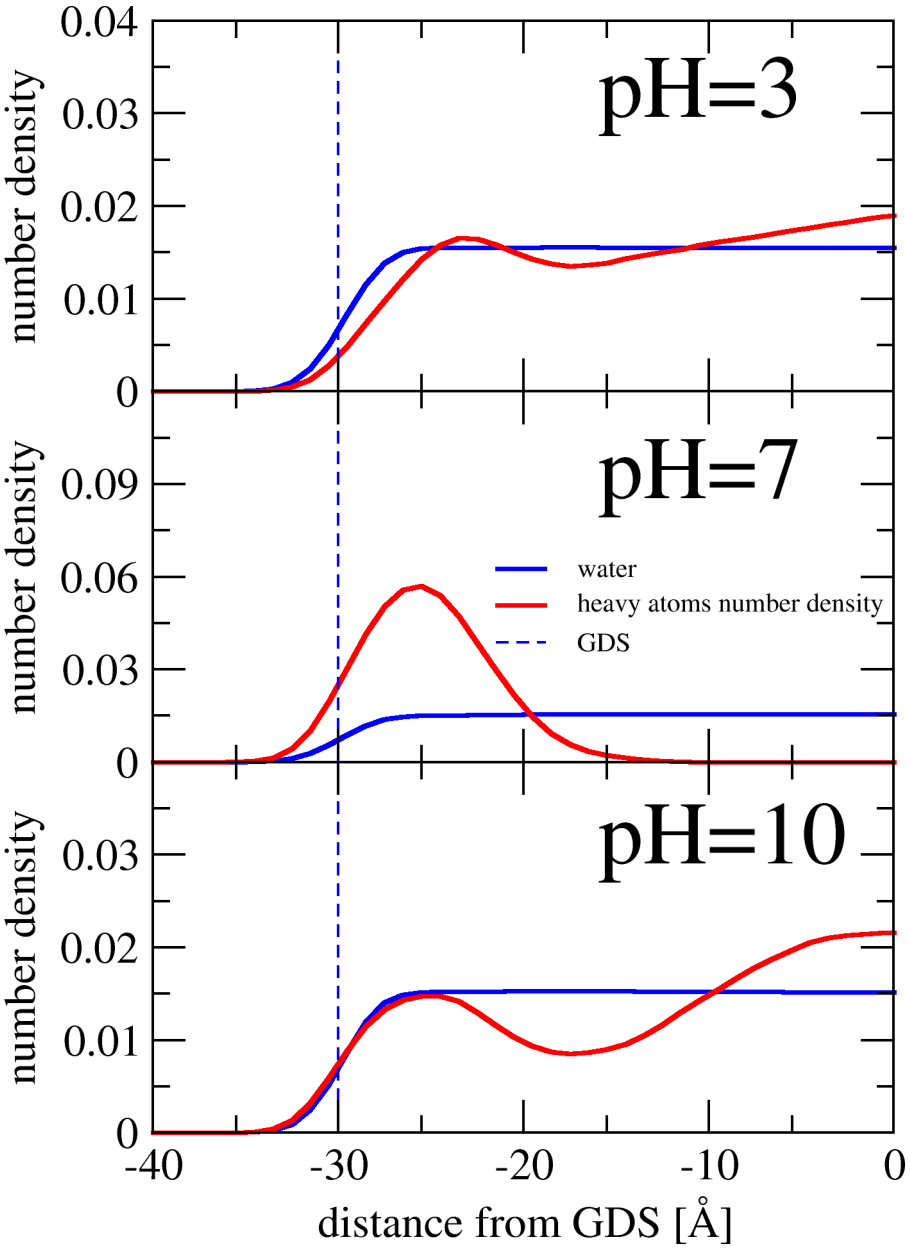
pH=3
pH=7
pH=10
number density
0.04
0.03
0.02
0.01
0
0.09
0.06
0.03
water
heavy atoms number density
GDS
-40
-30
-20
-10
0
distance from GDS [Å]

Figure 8

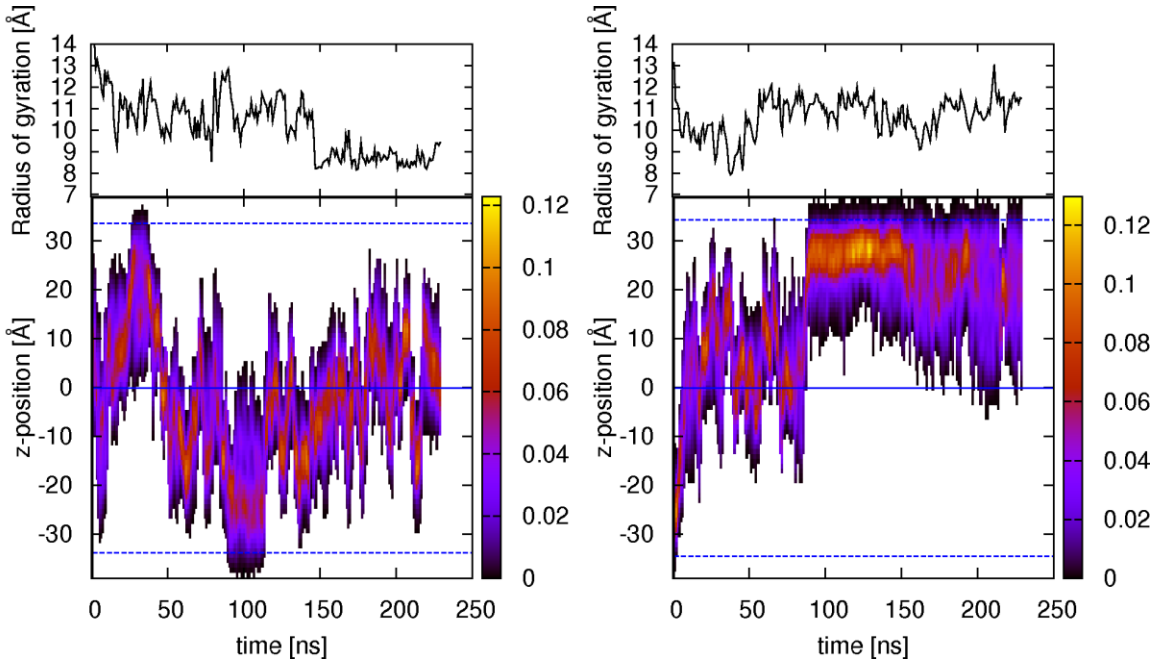
Radius of gyration [Å]
z-position [Å]
time [ns]
0
50
100
150
200
250
0.12
0.1
0.08
0.06
0.04
0.02
0

Figure 9

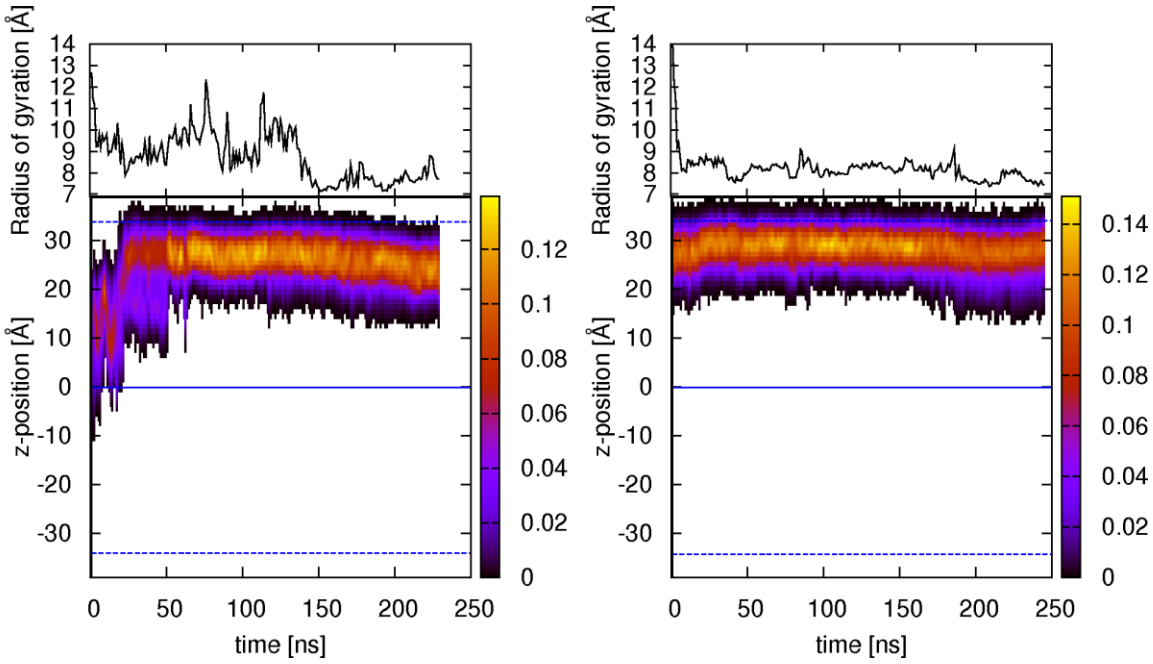
Radius of gyration [Å]
z-position [Å]
time [ns]
0
50
100
150
200
250
0.12
0.1
0.08
0.06
0.04
0.02
0.14

Figure 10

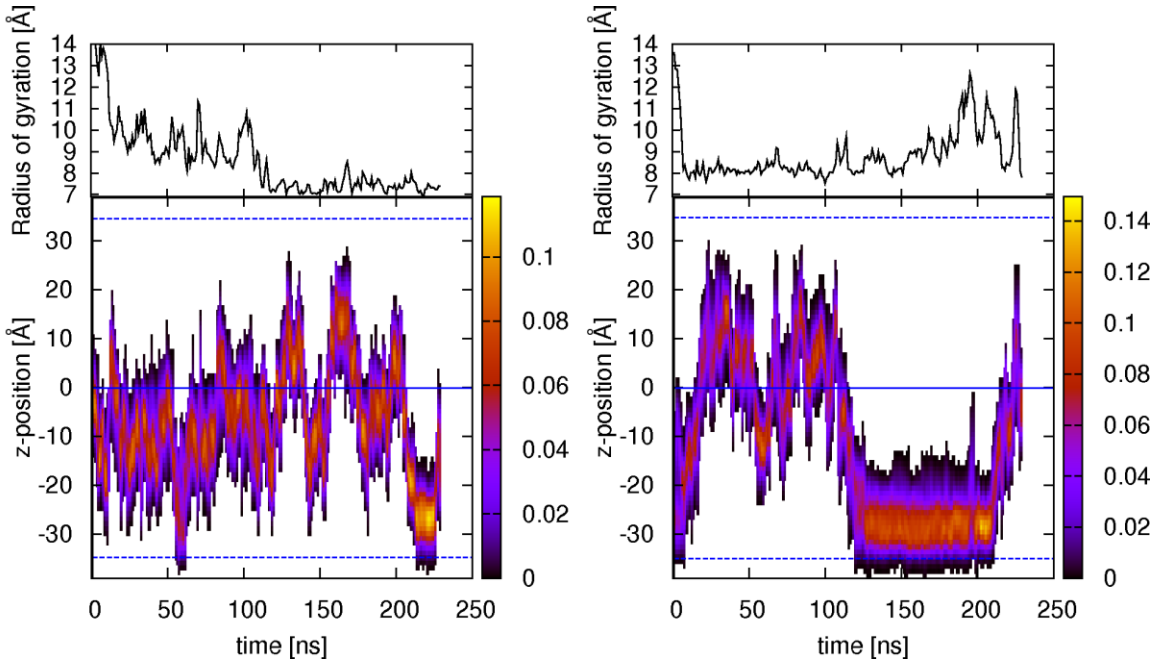
Radius of gyration [Å]
z-position [Å]
time [ns]
0
50
100
150
200
250
0.1
0.08
0.06
0.04
0.02
0
0.14
0.12

Figure 11

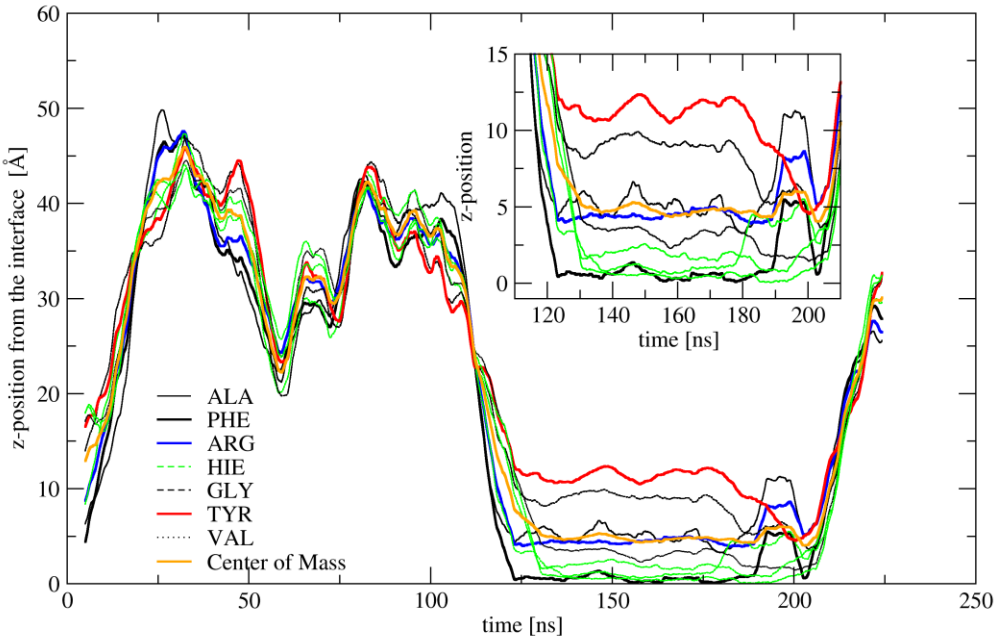
z-position from the interface [Å]
time [ns]
ALA
PHE
ARG
HIE
GLY
TYR
VAL
Center of Mass
z-position
time [ns]

References

(1) Selkoe, D. J. *Nature* **2003**, *426*, 900.

(2) Chiti, F.; Dobson, C. M. *Annual Review of Biochemistry* **2006**, *75*, 333.

(3) Bitan, G.; Kirkitadze, M. D.; Lomakin, A.; Vollers, S. S.; Benedek, G. B.; Teplow, D. B. *Proceedings of the National Academy of Sciences of the United States of America* **2003**, *100*, 330.

(4) Shanmugam, G.; Jayakumar, R. *Biopolymers* **2004**, *76*, 421.

(5) Triulzi, R. C.; Li, C. Q.; Naistat, D.; Orbulescu, J.; Leblanc, R. M. *Journal of Physical Chemistry C* **2007**, *111*, 4661.

(6) Strodel, B.; Lee, J. W. L.; Whittleston, C. S.; Wales, D. J. *Journal of the American Chemical Society* **2010**, *132*, 13300.

(7) Petersen, P. B.; Saykally, R. J. *Journal of Physical Chemistry B* **2006**, *110*, 14060.

(8) Petersen, P. B.; Saykally, R. J. *Annual Review of Physical Chemistry* **2006**, *57*, 333.

(9) Rinuy, J.; Brevet, P. F.; Girault, H. H. *Biophysical Journal* **1999**, *77*, 3350.

(10) Petralli-Mallow, T. P.; Plant, A. L.; Lewis, M. L.; Hicks, J. M. *Langmuir* **2000**, *16*, 5960.

(11) Salafsky, J. S.; Eisenthal, K. B. *Journal of Physical Chemistry B* **2000**, *104*, 7752.

(12) Perrenoud-Rinuy, J.; Brevet, P. F.; Girault, H. H. *Physical Chemistry Chemical Physics* **2002**, *4*, 4774.

(13) Mitchell, S. A.; McAloney, R. A. *Journal of Physical Chemistry B* **2004**, *108*, 1020.

(14) Smiley, B. L.; Vogel, V. *Journal of Chemical Physics* **1995**, *103*, 3140.

(15) Crawford, M. J.; Haslam, S.; Probert, J. M.; Gruzdkov, Y. A.; Frey, J. G. *Chemical Physics Letters* **1994**, *230*, 260.

(16) Salafsky, J. S. *Journal of Chemical Physics* **2006**, *125*.

(17) Petrallimallow, T.; Wong, T. M.; Byers, J. D.; Yee, H. I.; Hicks, J. M. *Journal of Physical Chemistry* **1993**, *97*, 1383.

(18) Polizzi, M. A.; Plocinik, R. M.; Simpson, G. J. *Journal of the American Chemical Society* **2004**, *126*, 5001.

(19) Nichols, M. R.; Moss, M. A.; Reed, D. K.; Hoh, J. H.; Rosenberry, T. L. *Biochemistry* **2005**, *44*, 165.

(20) Ambroggio, E. E.; Kim, D. H.; Separovic, F.; Barrow, C. J.; Barnham, K. J.; Bagatolli, L. A.; Fidelio, G. D. *Biophysical Journal* **2005**, *88*, 2706.

(21) Maltseva, E.; Kerth, A.; Blume, A.; Mohwald, H.; Brezesinski, G. *Chembiochem* **2005**, *6*, 1817.

(22) Brezesinski, G.; Maltseva, E.; Mohwald, H. *Zeitschrift Fur Physikalische Chemie-International Journal of Research in Physical Chemistry & Chemical Physics* **2007**, *221*, 95.

(23) Schladitz, C.; Vieira, E. P.; Hermel, H.; Mohwald, H. *Biophysical Journal* **1999**, *77*, 3305.

(24) Lemkul, J. A.; Bevan, D. R. *Biochemistry* **2010**, *49*, 3935.

(25) Lemkul, J. A.; Bevan, D. R. *Febs Journal* **2009**, *276*, 3060.

(26) Fu, Z. M.; Luo, Y.; Derreumaux, P.; Wei, G. H. *Biophysical Journal* **2009**, *97*, 1795.

(27) Wang, Q. M.; Zhao, J.; Yu, X. A.; Zhao, C.; Li, L. Y.; Zheng, J. *Langmuir* **2010**, *26*, 12722.

(28) Wu, C.; Biancalana, M.; Koide, S.; Shea, J. E. *Journal of Molecular Biology* **2009**, *394*, 627.

(29) Davis, C. H.; Berkowitz, M. L. *Proteins-Structure Function and Bioinformatics*, *78*, 2533.

(30) Knecht, V. *Journal of Physical Chemistry B* **2008**, *112*, 9476.

(31) Knecht, V.; Mohwald, H.; Lipowsky, R. *Journal of Physical Chemistry B* **2007**, *111*, 4161.

(32) Kwan, A. H.; Macindoe, I.; Vukasin, P. V.; Morris, V. K.; Kass, I.; Gupte, R.; Mark, A. E.; Templeton, M. D.; Mackay, J. P.; Sunde, M. *Journal of Molecular Biology* **2008**, *382*, 708.

(33) *CRC Handbook of Chemistry and Physics*; Haynes, W. M., Ed.; CRC Press: New York, 2010.

(34) Li, H.; Robertson, A. D.; Jensen, J. H. *Proteins* **2005**, *61*, 704.

(35) Wang, J. M.; Wolf, R. M.; Caldwell, J. W.; Kollman, P. A.; Case, D. A. *Journal of Computational Chemistry* **2004**, *25*, 1157.

(36) Berendsen, H. J. C.; Grigera, J. R.; Straatsma, T. P. *Journal of Physical Chemistry* **1987**, *91*, 6269.

(37) Smith, D. E.; Dang, L. X. *Journal of Chemical Physics* **1994**, *100*, 3757.

(38) Case, D. A. D., T. A.; Cheatham, III, T. E; Simmerling, C. L.; Wang, J.; Duke, R. E.; Luo, R.; Crowley, M.; Walker, R. C.; Zhang, W.; Merz, K. M.;Wang, B.; Hayik, S.; Roitberg, A.; Seabra, G.; Kolossvary, I.;Wong, K. F.; Paesani, F.; Vanicek, J.;Wu, X.; Brozell, S. R.; Steinbrecher, T.; Gohlke, H.; Yang, L.; Tan, C.; Mongan, J.; Hornak, V.; Cui, G.; Mathews, D. H.; Seetin, M. G.; Sagui, C.; Babin, V.; Kollman, P. A. Amber 10; Amber 10, University of California, San Francisco: San Francisco, 2008.

(39) Essmann, U.; Perera, L.; Berkowitz, M. L.; Darden, T.; Lee, H.; Pedersen, L. G. *Journal of Chemical Physics* **1995**, *103*, 8577.

(40) Berendsen, H. J. C.; Postma, J. P. M.; Vangunsteren, W. F.; Dinola, A.; Haak, J. R. *Journal of Chemical Physics* **1984**, *81*, 3684.

(41) Ryckaert, J. P.; Ciccotti, G.; Berendsen, H. J. C. *Journal of Computational Physics* **1977**, *23*, 327.

(42) Volkov, A. G.; Dreamer, D. W.; Tanelian, D. L.; Markins, V. S. *Liquid Interfaces in Chemistry and Biology*; Wiley-Interscience: New York, 1998.

(43) Petersen, P. B.; Saykally, R. J. *J. Phys. Chem. B* **2005**, *109*, 7976.

(44) Petersen, M. K.; Iyengar, S. S.; Day, T. J. F.; Voth, G. A. *Journal of Physical Chemistry B* **2004**, *108*, 14804.

(45) Buch, V.; Milet, A.; Vacha, R.; Jungwirth, P.; Devlin, J. P. *Proceedings of the National Academy of Sciences of the United States of America* **2007**, *104*, 7342.

(46) Petersen, P. B.; Saykally, R. J., in preparation.

(47) Petty, S. A.; Decatur, S. M. *Proceedings of the National Academy of Sciences of the United States of America* **2005**, *102*, 14272.

(48) Xu, R.; Dickinson, E.; Murray, B. S. *Langmuir* **2007**, *23*, 5005.

Table of Contents Graphic